JOURNAL OF MATERIALS SCIENCE 21 (1986) 2689–2696

The identification of thin amorphous films at grain-boundaries in Al_2O_3

Y. KOUH SIMPSON, C. B. CARTER
Department of Materials Science and Engineering, Bard Hall, Cornell University, Ithaca, New York 14853, USA

K. J. MORRISSEY
DuPont de Nemours Co., Experimental Research Station, Wilmington, Delaware, USA

P. ANGELINI, J. BENTLEY
Metals and Ceramics Division, Oak Ridge National Laboratory, Oak Ridge, Tennessee 37831, USA

The presence of amorphous grain-boundary phases in ceramic materials can significantly influence their properties. Such grain-boundary films can be identified by the dark-field diffuse scattering technique, the Fresnel fringe technique, and analytical electron microscopy (energy-dispersive spectroscopy). However, spectrum artefacts can present major problems for the use of such techniques. Specifically, grain-boundary grooving, surface damage of the specimen and silicon contamination are shown experimentally to arise from ion-milling during the preparation of TEM specimens. It is experimentally shown that, with the above techniques, these artefacts can cause grain-boundaries in commercial alumina specimens to appear to contain glassy phases. The ambiguity in interpreting the results from the use of each of these techniques is discussed in detail.

1. Introduction

In polycrystalline ceramic materials, grain-boundaries may be structured similar to boundaries in metals [1, 2] or they may contain an intergranular, amorphous (glassy) phase [3–5]. The structure may also involve a mixture of these two interface types [6]. The properties of such materials will clearly depend on the actual structure of the grain-boundaries; if an amorphous phase is present at the interface the response of the material to an applied stress may be governed by the properties of the amorphous film.

Several recent papers [7–11] have reported observations made using transmission electron microscopy (TEM) on faceted grain-boundaries in alumina, where the observations are interpreted as showing that a glassy phase is present at the grain-boundary. In particular it has been proposed that all faceted grain-boundaries in alumina, with the exception of the basal twin boundary, contain this amorphous intergranular phase [7]. This general claim has been disputed by Morrissey and Carter [12, 13] who showed experimentally that other special, structured interfaces do occur in alumina and that these structured interfaces are usually faceted.

There are several TEM techniques which may be used to identify glassy phases at grain-boundaries and these have been reviewed by Clarke [14]. They include the dark-field diffuse scattering technique, the Fresnel fringe technique and high resolution TEM (HRTEM). Analytical electron microscopy (AEM) utilizing energy-dispersive X-ray spectroscopy (EDS) can be used to provide chemical analysis of the interfacial region. However, one of the problems in actually using these techniques to identify very thin glassy films of $\lesssim 5$ nm width is that artefacts may be produced during specimen preparation, and these artefacts can influence both the actual observations and the interpretation. For example, possible artefacts resulting from ion-milling are preferential grooving of the grain-boundary region, ion-beam damage of the surface layer and silicon contamination.

The purpose of this paper is to discuss the application of the three techniques, namely the dark-field diffuse scattering method, the Fresnel fringe technique and X-ray microanalysis, to grain-boundaries in commercial polycrystalline aluminas, and in particular to show experimentally how the artefacts produced during ion-milling may give a misleading impression of the nature of the interface.

2. Experimental procedure

The observations discussed in this paper were made on polycrystalline alumina specimens of McDanel 998 and Coors 998 commercial aluminas. It is emphasized that the materials were chosen because they are known to contain a wide range of grain-boundaries [12, 13], and not in order to characterize or compare the individual materials. The TEM specimens from these materials were prepared by first mechanically grinding 3 mm discs to 50 μm thickness and then subsequently ion-milling the discs to perforation. TEM studies were performed with a Jeol 200 CX operating at 200 kV and a Jeol 1200 EX operating at 120 kV. The AEM study has been accomplished with a Philips EM 400T

0022–2461/86 $03.00 + .12

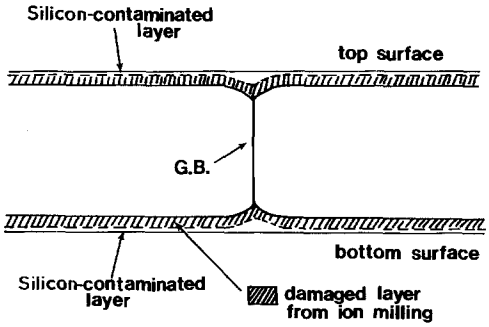

Figure 1 A schematic diagram of a grooved grain-boundary (G.B.). Surface damage of the specimen and silicon contamination are also present due to the ion-milling process.

scanning transmission electron microscope (STEM) equipped with a field-emission gun (FEG) and an EDAX 9100/70 EDS system.

3. Results and discussion

3.1. Grain-boundary grooving due to ion-milling

Grain-boundary grooving is a phenomenon which is often observed experimentally in TEM specimens that have been ion-milled, although care is required in identifying this effect since its magnitude is small. The preferential milling which causes grooving at grain-boundaries occurs because the atomic bonding is weaker at the grain-boundaries than in the perfect crystalline regions inside the grains. Rühle [15] has previously shown experimentally by subsequent shadowing with gold that the grain-boundaries in polycrystalline alumina can be grooved after ion-milling. This result has been confirmed in this study. However, as found by Rühle, not all grain-boundaries in alumina are grooved. This variability is as expected, since the grain-boundary grooving must depend on such variables as the orientation of the grain-boundary relative to the surface of the specimen, the grain-boundary character, and the grain-boundary configuration. Thus, for example, a low-energy grain-boundary such as a basal twin boundary in alumina might not be expected to groove.

Fig. 1 shows a schematic diagram of a grooved grain-boundary. In this diagram, two other possible effects of ion-milling mentioned above, the damaged non-crystalline region on the surface of the specimen and the silicon contamination, are illustrated. According to the recent review by Howitt [16], the damaged region on each surface of the ion-thinned alumina specimen can be as thick as 10 nm. Two examples of grain-boundary grooving are shown in Figs 2 and 3. The high-resolution image of germanium is included in order to show that grain-boundary grooving produced by ion-milling can occur even when it is known that no glassy film is present at the grain-boundary. The presence of a thin, glassy film at the grain-boundary in a high-resolution image could obscure the grooving effect. Fig. 3 is a typical bright-field image of the type of grooved grain-boundary often observed in these polycrystalline alumina specimens.

3.2. Dark-field diffuse scattering

Fig. 4 illustrates schematically the principal feature of the dark-field diffuse scattering technique for imaging an amorphous film in an edge-on grain-boundary. If amorphous material is present, a diffuse ring will be present around the transmitted beam. In practice this ring can only be recorded photographically when a large volume of amorphous material is present, as can occur at a three-grain junction. The objective aperture is then placed on this ring, taking care to avoid any diffraction spots, particularly double-diffraction spots which may also be very weak. In the corresponding imaging mode, any amorphous material in the grain-boundary region which contributes to the diffuse

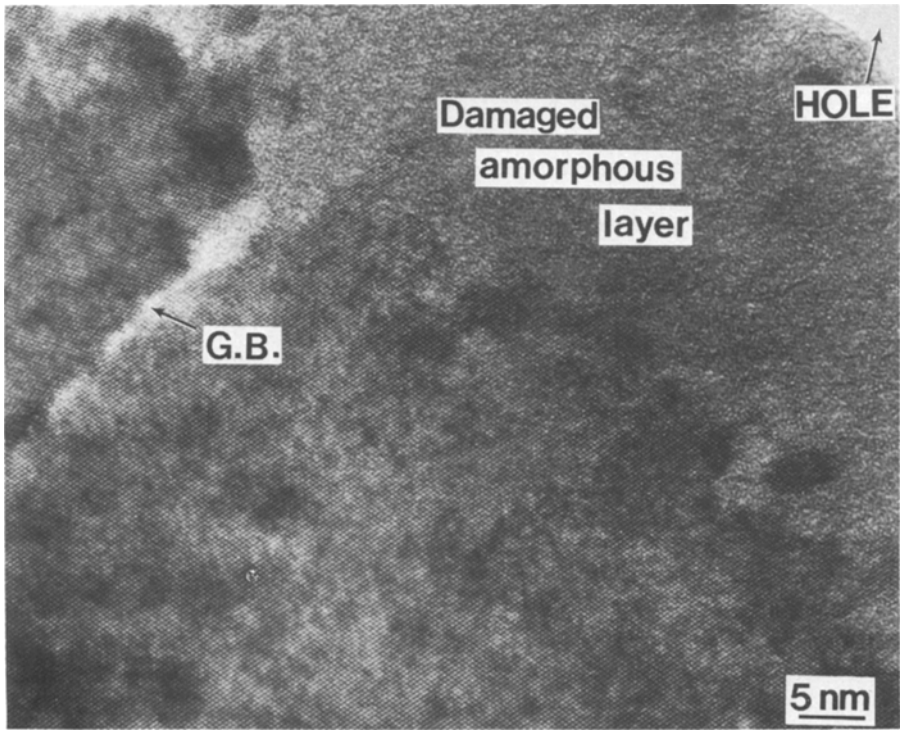

Figure 2 HRTEM image of a structured grain-boundary (G.B.) in germanium. The non-crystalline region near the edge of the hole is due to the damage produced by the ion-milling.

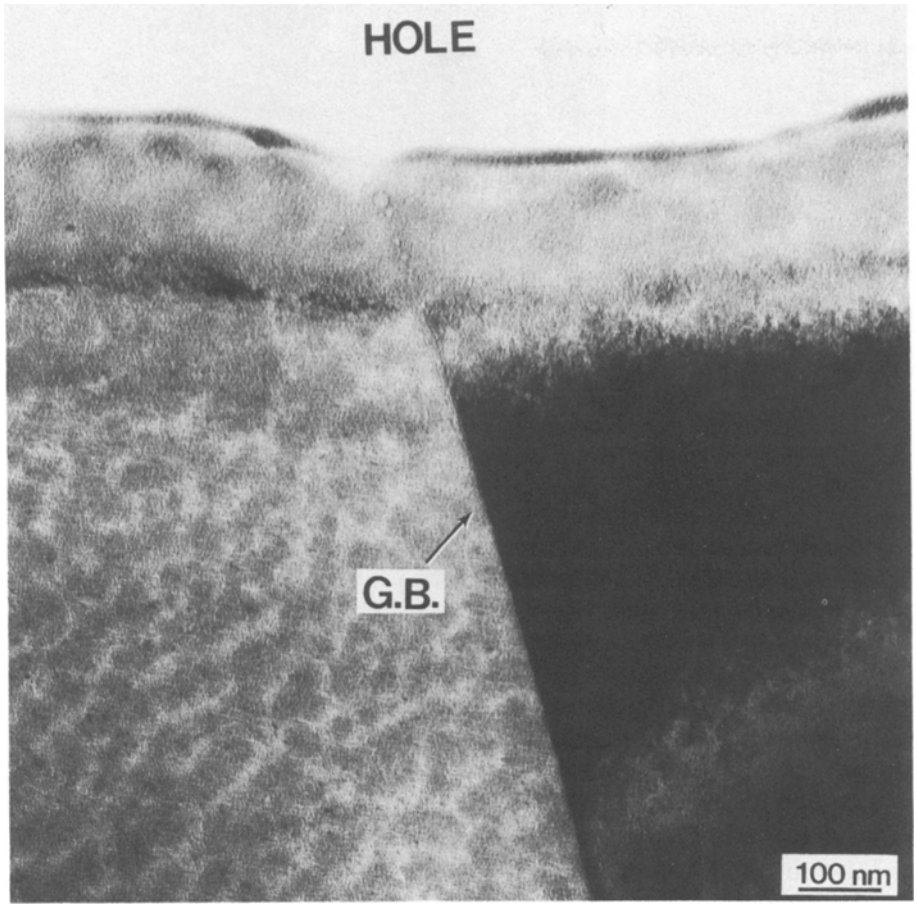

Figure 3 A bright-field image of a grooved grain-boundary (G.B.) in Al_2O_3.

scattered ring intensity will then cause this region to appear bright.

The bright line along such edge-on grain-boundaries is interpreted as evidence for an amorphous phase present in the grain-boundary. It can be shown, however, that this simple interpretation may be misleading. As illustrated in Figs 5a and b, a grain-boundary which appears as a bright line against a dark background in the edge-on orientation may appear as two distinct bright lines at the grain-boundary when the grain-boundary is tilted. In the tilted condition, the intensity between the two bright lines in the dark-field, diffuse-scattering image is the same as in the rest of the image. The observation of the two lines instead of the one broad fringe which would be expected if an amorphous film were actually present at the grain-boundary

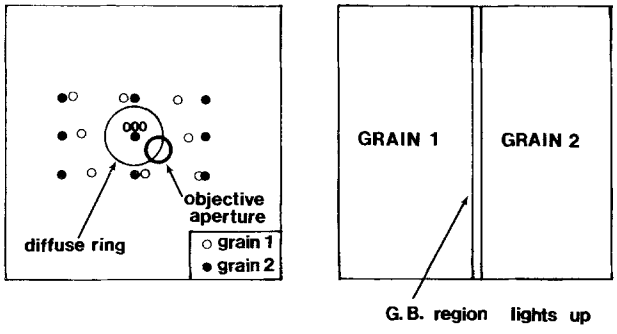

Figure 4 A schematic illustration of the dark-field diffuse scattering technique. The region that contributes to the diffuse ring intensity around the transmitted beam appears bright in the dark-field image. G.B. = grain-boundary.

can be explained, for example, by the diagram for the tilted geometry shown in Fig. 6. This diagram is the same as that shown in Fig. 1 except that the grain-boundary is now tilted, so that it is no longer viewed edge-on with respect to the electron beam. If a clean, structured grain-boundary is grooved and the grooves are filled with amorphous material, then when the specimen is tilted the projected image of the grain-boundary will show higher intensity at the two regions corresponding to the top and bottom of the specimen. The effect observed in Figs 5a and b is therefore associated with amorphous material filling the grooves and giving rise to diffuse scattering. This material may be either a contamination layer or the carbon coating.

It might be argued that the grain-boundary did not appear uniformly bright because the aperture used to form the image in Fig. 5b was not correctly positioned. The interpretation illustrated above by Fig. 6 is, however, confirmed by Fig. 7, which shows two distinct lines at a tilted grain-boundary near the pocket of amorphous material at the three-grain junction. When tilted the three-grain junction shows a uniform intensity along the thickness of the specimen, whereas the grain-boundary region shows two white lines. If the grain-boundary were totally wet with the glassy phase, it would show the same even intensity along the thickness of the foil. This type of contrast has been observed during the study of grain-boundaries in Si_3N_4 which were known to contain an amorphous film by the use of HRTEM [4]. Two final points should be noted. In a dark-field, diffuse-scattering image the grains are never completely dark as can be

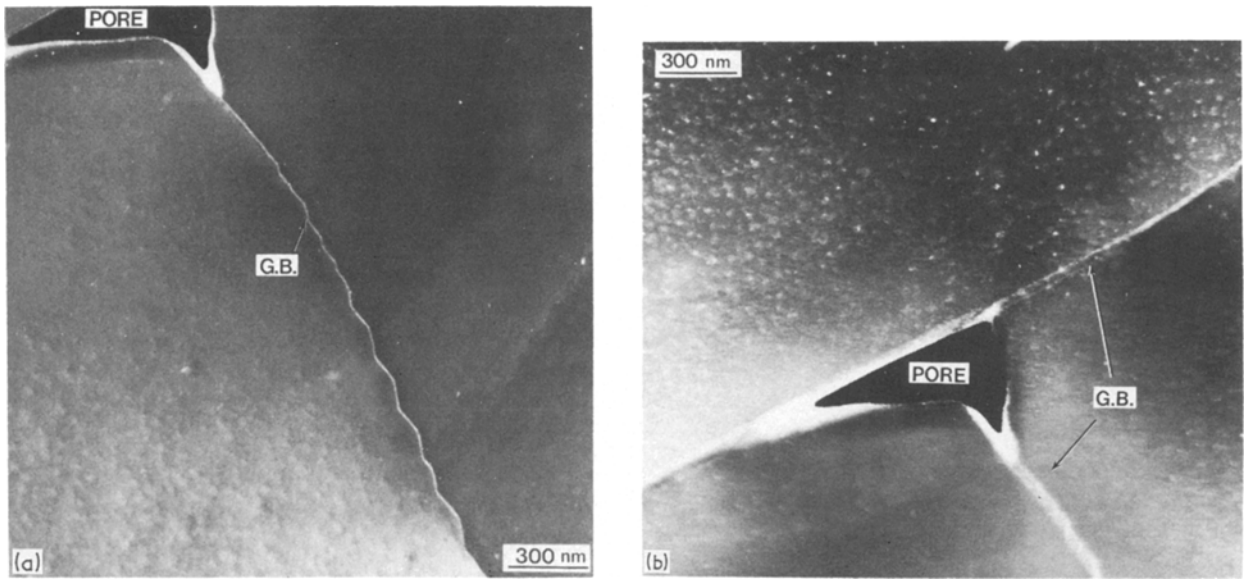

Figure 5 Dark-field images formed using diffuse scattering: (a) edge-on grain-boundary (G.B.) in Al_2O_3, (b) the same region when tilted; the grain-boundary now shows two bright lines.

clearly appreciated by viewing a pore. This background contrast is due to a combination of the presence of the damaged layer [17], the contamination layer present on the surface of the specimen, and the necessary carbon coating. If weak diffraction spots that arise by double diffraction are included in the objective aperture, the tilted grain-boundary can appear uniformly bright compared with the background intensity.

3.3. Fresnel fringe technique

This technique, as illustrated in Fig. 8, can be used to identify a local change in inner potential at the grain-boundary. Images of Fresnel fringes at an interface are recorded for different defocus conditions with the grain-boundary oriented parallel to the electron beam. The defocus values indicated in Fig. 8 are typical. The magnification and change in mean inner potential dictate the actual value to be used. The Fresnel fringes result from the different phase shifts experienced by the electron beam as it passes through materials of different mean inner potentials. Such Fresnel fringe contrast will be found when an amorphous film is present at the grain-boundary, when there is a thin gap between the grains, or when the grain-boundary is structured. Rühle and Sass [18] reported observations of Fresnel fringes when individual dislocations in NiO grain-boundaries were viewed end-on. Boothroyd and Stobbs [19] reported a similar effect for dislocations inclined to the electron beam. Observations of Fresnel fringes have been reported for twin boundaries in both copper [20] and spinel [21]. An example of a high-angle, structured grain-boundary in alumina giving rise to such Fresnel fringes is shown in Fig. 9. The difference in the local mean inner potential occurs because of the lower density at the core of the dislocations present in the structured grain-boundary; the inner potential may also be influenced by segregation of impurities to these cores. The Fresnel effect has also been observed when small voids or cavities are present in a TEM sample [22, 23] or when there are steps on the surface [24]. It may therefore be concluded that Fresnel fringes can be observed at an interface whenever the electron beam experiences a different mean inner potential. This result holds independently of whether the local change in inner potential is due either to a local change in composition or to a local change in thickness.

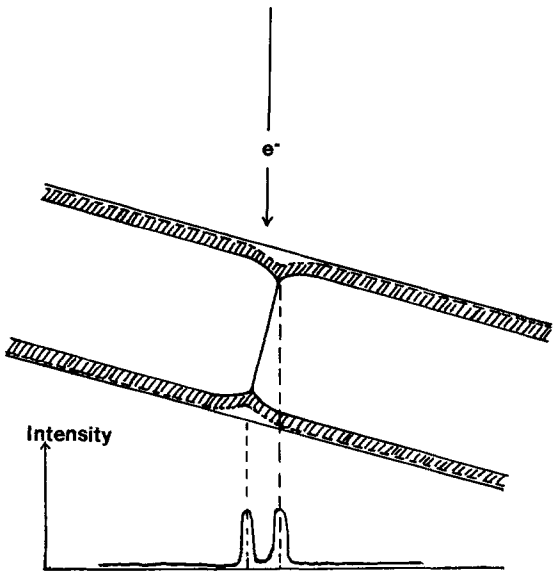

Figure 6 A schematic diagram of a grooved grain-boundary in a tilted geometry. The observation of two bright lines can be due to the amorphous materials filling the grooves at the top and bottom of the specimen at the grain-boundary.

3.4. Microanalysis by EDS

This technique uses EDS X-ray microanalysis, with a small electron probe usually obtained in the scanning transmission electron microscopy (STEM) imaging mode, to obtain information on the composition of grain-boundaries. The geometry for the EDS technique is shown schematically in Fig. 10. The characteristic X-rays from the grain-boundary region give quantitative information on the concentration of

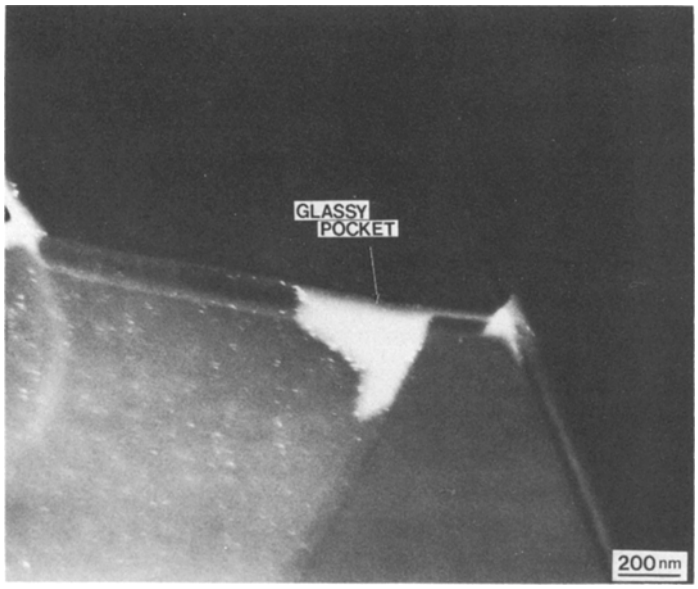

Figure 7 A dark-field image formed using diffuse scattering of a region near a pore in Al_2O_3 (tilted condition). The pore shows an even intensity along its thickness, but the grain-boundaries show two distinct bright lines.

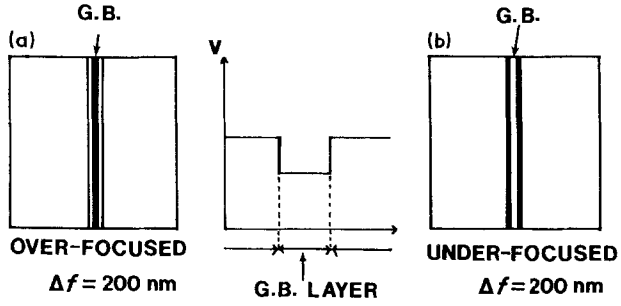

Figure 8 A schematic illustration of images formed using the Fresnel fringe technique. When the defocus value is changed, the contrast of the Fresnel fringes at the grain-boundary (G.B.) reverses.

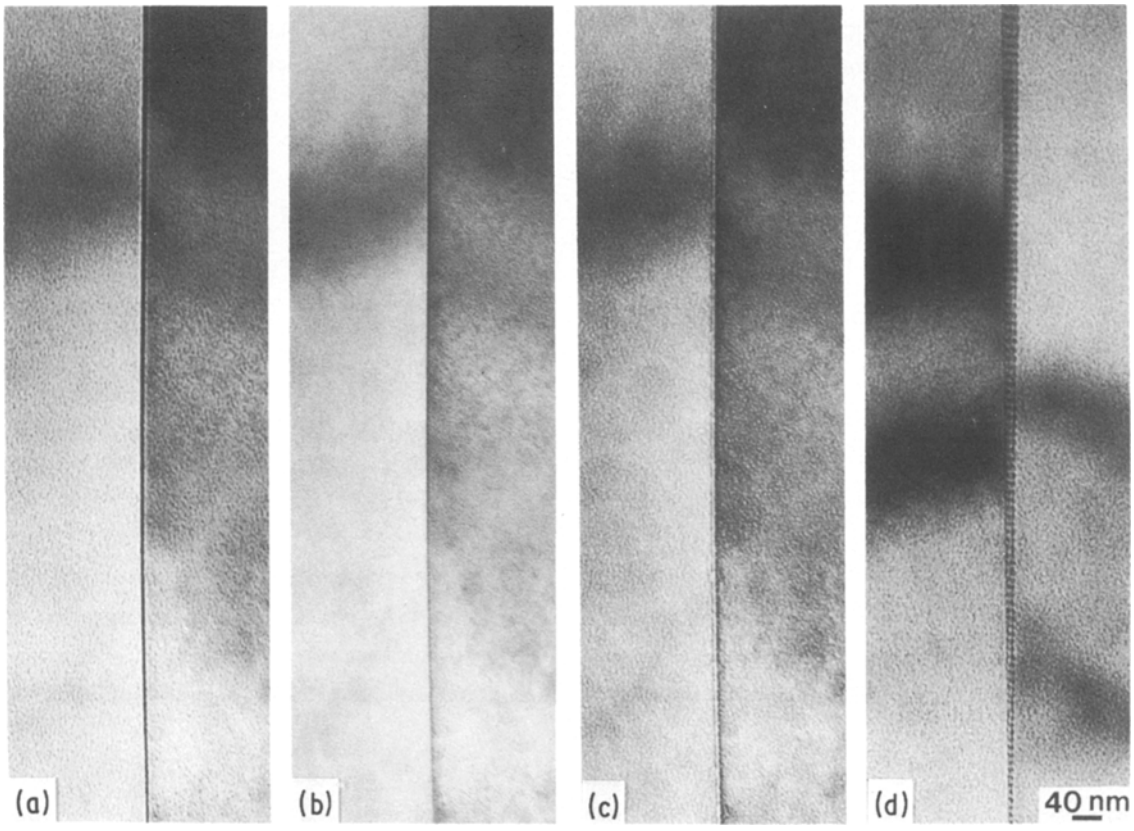

Figure 9 A structured grain-boundary in Al_2O_3 showing the Fresnel fringes at (a) the over-focused, (b) the focused and (c) the under-focused conditions when viewed edge-on. (d) When the grain-boundary is tilted by 11° the interface shows dislocation contrast.

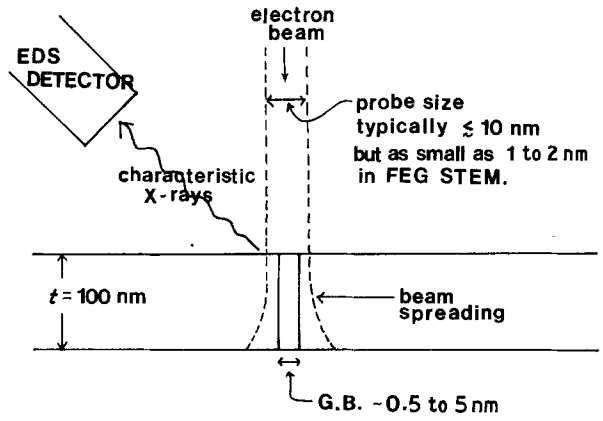

Figure 10 A schematic diagram showing the AEM (EDS) technique. FEG = field-emission gun, G.B. = grain-boundary.

elements present in that region. This technique cannot, however, distinguish whether these elements are present as solute atoms segregated to structured grain-boundaries, or if they are present in a film of amorphous material, or if they are present in a groove at the surface. The quantitative analysis of the exact composition of the grain-boundary region is also difficult because the electron probe diameter is usually larger than the grain-boundary width. Furthermore, beam spreading occurs within the foil so that the chemical information obtained from the grain-boundary region does not originate only at the grain-boundary region, but may be affected by the grains on either side of the grain-boundary [25].

The spectra shown in Fig. 11 were obtained from an alumina specimen which had been thinned with the use of an ion-miller operating with a silicone-based diffusion pump oil. It should be noted that most commercial ion-millers use such diffusion pump oil since it satisfactorily meets the performance requirements for normal use of an ion-miller to prepare thin TEM foils; i.e. the oil is economical and resistant to cracking [26]. The presence of a silicon-contaminated layer covering the specimen is clearly indicated by the spectrum in Fig. 11a, which was recorded with the beam located at the centre of a grain. The solubility of silicon in alumina is well below the detectability limit of the EDS technique (~0.1 wt% [27]). Hence it can be concluded that a contamination layer containing silicon exists on the specimen. Argon is implanted during the ion-milling process and gives rise to the argon peak which is clearly seen in every spectrum recorded from this specimen. The detection of argon has previously been reported [28–30]. Fig. 11b was obtained from a grain-boundary associated with the grain of Fig. 11a. In addition to silicon this spectrum shows the presence of calcium. Calcium segregation at structured grain-boundaries is a well-known phenomenon [31–34] and thus, in itself, is not evidence for the presence of an amorphous phase.

Figs 12a and b show spectra taken from the same specimen after further thinning in a different ion-miller. The spectrum taken from the matrix no longer shows the presence of silicon. Argon is still detected, although at a lower concentration. The spectrum in Fig. 12b, taken from the associated grain-boundary, shows a much smaller concentration of silicon than previously detected at the grain-boundary (Fig. 11b). It is strongly suggested that a silicon contamination layer can arise due to the use of a silicone-based diffusion pump oil in an ion-miller. It might be noted that at least one manufacturer has now replaced the diffusion pump entirely with a turbo-molecular pump. It is presently not clear whether the silicon contamination layer builds up on the specimen during the ion-milling, or after this process while the specimen remains in the ion-miller. Silicon contamination can also occur in the microscope if beam-sensitive materials containing silicon have been examined recently [35].

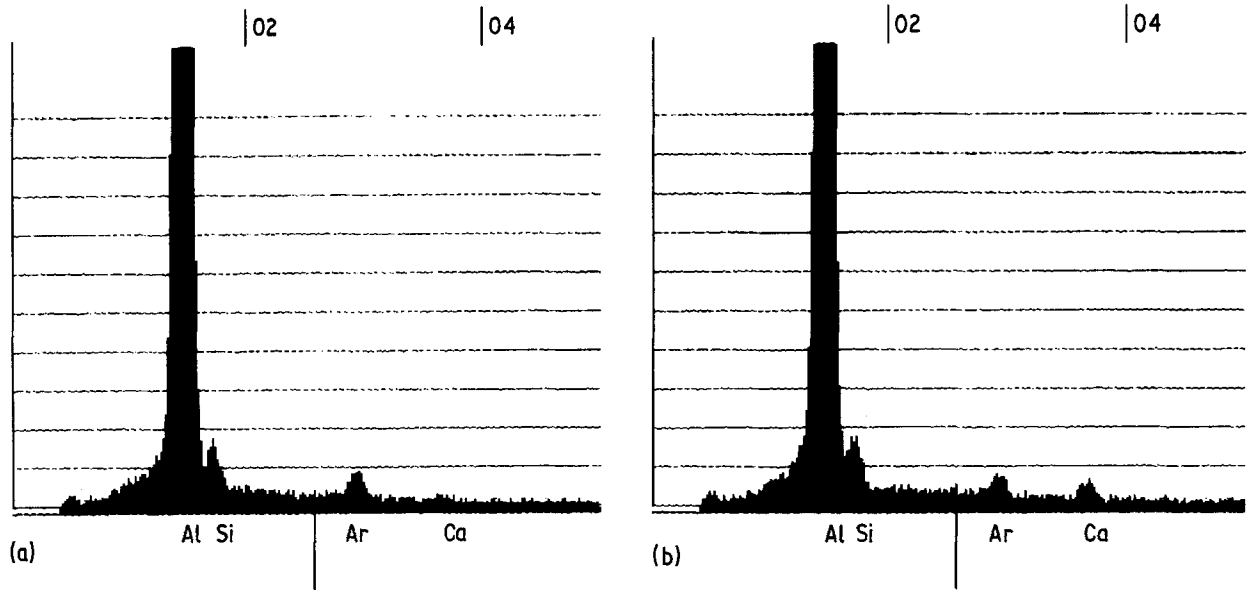

Figure 11 (a) A spectrum taken from the middle of a grain in Al_2O_3 which has been ion-milled in an instrument using a silicone-based diffusion pump oil. The silicon peak shown indicates the presence of silicon at the level exceeding the silicon solubility in Al_2O_3 matrix. Argon is also present. (b) A spectrum taken from an associated grain-boundary near the grain in (a). In addition to silicon and argon, calcium is also present.

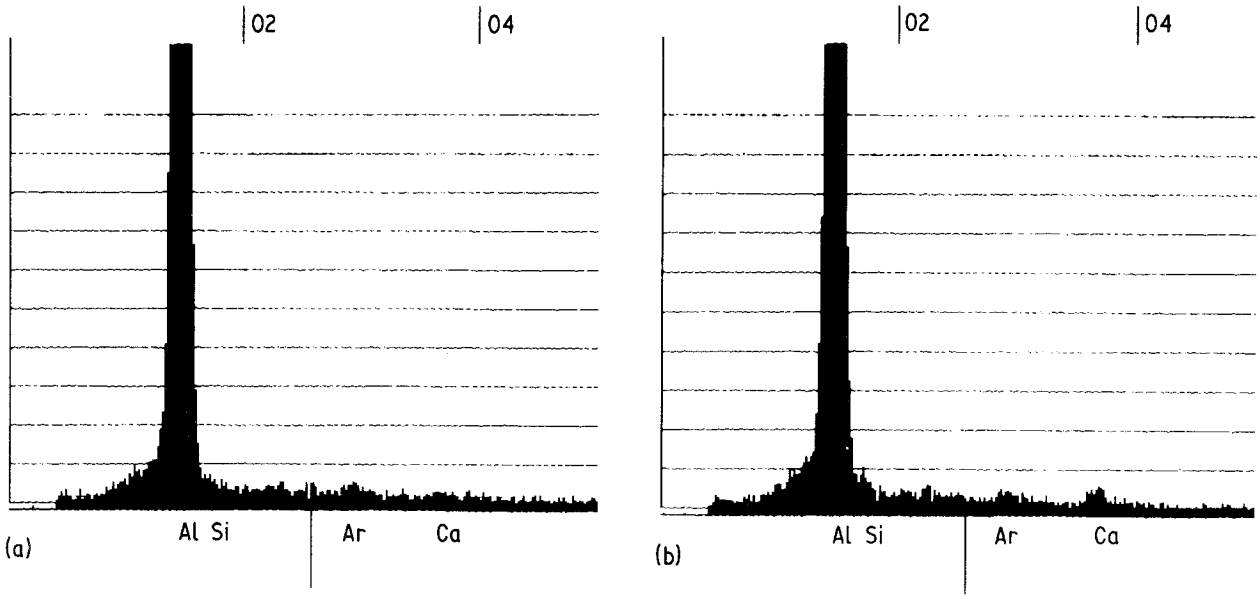

Figure 12 (a) A specimen taken from the middle of a grain after re-milling in a different ion-miller using non-silicone based diffusion pump oil. There is effectively no silicon, and the argon peak is much lower compared to Fig. 11a. (b) A spectrum taken from an associated grain-boundary near the grain in (a). The silicon level is much lower than that at grain-boundaries before re-milling.

It should also be noted that silicon has been found in the carbon films of extraction replicas of other materials. An evaporator with silicon-based diffusion pump oil was used. The effect could be reduced by allowing a larger pump-out time (lower pressure) before the carbon arc was struck. A better solution is again to use a non-silicone containing diffusion pump oil, such as a polyfluorinated ether.

4. Conclusions

It has been shown experimentally in this paper that many grain-boundaries in alumina form grooves during ion-milling while preparing the TEM specimen. This grooving depends on variables such as the grain-boundary orientation relative to the specimen surface, the grain-boundary character and the grain-boundary configuration. Along with the grain-boundary grooving, surface damage of the specimen and silicon contamination can occur during both the ion-milling process and the carbon-coating process. In the presence of such artefacts produced by the specimen preparation, experimental evidence suggests that the use of the dark-field, diffuse scattering method, the Fresnel fringe technique and the EDS analysis to identify glassy phases at grain-boundaries can give misleading results. These techniques, by themselves, cannot be used to identify conclusively the presence of glassy phases at grain-boundaries. Whenever possible HRTEM must be employed in conjunction with these techniques.

Acknowledgements

The authors would like to thank Dr W. Skrotzki for the use of Fig. 2 and Dr E. L. Hall for helpful discussions on the subject of the grain-boundary segregation in MgO. They also thank Mr Ray Coles for maintaining the microscopes at Cornell. This research is supported by the Department of Energy under grant No. DE-FG02-84ER45092 at Cornell, and by the Division of Materials Sciences, US Department of Energy under contract No, DE-AC05-84OR21400 with Martin Marietta Energy Systems, Inc., and under contract No. DE-76-C-05-0033 with Oak Ridge Associated Universities (SHaRE program).

References

1. R. W. BALLUFFI (editor), "Grain Boundary Structure and Kinetics" (ASM, Ohio, 1980).
2. G. A. CHADWICK and D. A. SMITH (editors), "Grain Boundary Structure and Properties" (Academic Press, London, 1976).
3. D. R. CLARKE and G. THOMAS, *J. Amer. Ceram. Soc.* **60**(11–12) (1977) 491.
4. O. L. KRIVANEK, T. M. SHAW and G. THOMAS, *J. Appl. Phys.* **50** (1979) 4223.
5. L. K. V. LOU, T. E. MITCHELL and A. H. HEUER, *J. Amer. Ceram. Soc.* **61**(9–10) (1978) 392.
6. C. B. CARTER and Z. ELGAT, *Adv. Ceram.* **6** (1983) 73.
7. S. C. HANSEN and D. S. PHILLIPS, *Phil. Mag. A.* **47**(2) (1983) 209.
8. *Idem, Adv. Ceram.* **6** (1983) 163.
9. D. S. PHILLIPS and Y. R. SHIUE, *ibid.* **10** (1984) 357.
10. C.-W. LI and W. D. KINGERY, *ibid.* **10** (1984) 368.
11. M. P. HARMER, *ibid.* **10** (1984) 679.
12. K. J. MORRISSEY and C. B. CARTER, *J. Amer. Ceram. Soc.* **67**(4) (1984) 292.
13. C. B. CARTER and K. J. MORRISSEY, *Adv. Ceram.* **10** (1984) 303.
14. D. R. CLARKE, *Ultramicroscopy* **4** (1979) 33.
15. M. RÜHLE, private communication (1985).
16. D. G. HOWITT, *J. Electr. Microsc. Tech.* **1**(4) (1984) 405.
17. N. W. JEPPS, T. F. PAGE and W. M. STOBBS, in "Grain Boundaries in Semiconductors" (Elsevier, Amsterdam, 1982) p. 45.
18. M. RÜHLE and S. L. SASS, *Phil. Mag. A.* **49**(6) (1984) 759.
19. C. B. BOOTHROYD and W. M. STOBBS, *Phil. Mag. A.* **49**(1) (1984) L5.
20. W. M. STOBBS and D. J. SMITH, in "Electron Microscopy and Analysis", Conference Series No. 61 (Institute of Physics, London, 1981) p. 373.
21. C. B. CARTER, Z. ELGAT and T. M. SHAW, in preparation.
22. M. RÜHLE and M. WILKENS, *Cryst. Lattice Defects* **6**

(1975) 129.
23. S. IIJIMA, *Optik.* **47**(4) (1977) 437.
24. C. BOULESTEIX, C. COLLIEX, C. MORY, D. RENARD and B. YANGUI, *J. Microsc. Spectrosc. Electron.* **3**(3) (1978) 185.
25. D. B. WILLIAMS, "Practical Analytical Electron Microscopy in Materials Science" (Philips Electron Optics Publishing Group, Mahwah, New Jersey, 1984) p. 82.
26. J. F. O'HANLON, "A Users Guide to Vacuum Technology" (Wiley, 1980) p. 195.
27. C. H. LEE and F. A. KRÖGER, *J. Amer. Ceram. Soc.* **68**(2) (1985) 92.
28. D. R. CLARKE, *ibid.* **63**(5–6) (1980) 339.
29. K. J. MORRISSEY and C. B. CARTER, in "Advances in Materials Characterization", edited by D. R. Rossington, R. A. Condraste and R. L. Snyder (Plenum, 1983) p. 297.
30. K. J. MORRISSEY, Y. KOUH and C. B. CARTER, in Proceedings of 41st EMSA Conference (San Francisco Press, San Francisco, 1983) p. 46.
31. W. C. JOHNSON, D. F. STEIN and R. W. RICE, in Proceedings of 4th Bolton Landing Conference (Claitors, Baton Rouge, Louisiana, 1974) p. 261.
32. W. C. JOHNSON and R. L. COBLE, *J. Amer. Ceram. Soc.* **61**(3–4) (1978) 110.
33. S. BAIK, D. E. FOWLER, J. M. BLAKELY and R. RAJ, *ibid.* **68**(5) (1985) 281.
34. W. D. KINGERY, T. MITAMURA, J. B. VANDER SANDE and E. L. HALL, *J. Mater. Sci. Lett.* **14** (1979) 1766.
35. J. T. SCHWARTZ, private communication (1985).

Received 29 July
and accepted 18 September 1985